A Tale of Two Forces: Simultaneous Chemical and Acoustic Propulsion of Bimetallic Micromotors

Wei Wang,[a] Wentao Duan,[b] Zexin Zhang,[c] Mei Sun,[a] Ayusman Sen,[b] and Thomas E. Mallouk[b,d,e*]

Supporting Information

1. Experimental details

Synthesis of microrods

Metallic microrods were grown electrochemically in anodic alumina membranes as described in previous reports.[1-3] Whatman Anapore membranes with a nominal pore size of 200 nm (actual pore diameter 300-350 nm) were used. By controlling the electrical current and time of the electrodeposition process, microrods of different lengths were prepared. Typically, a sacrificial silver segment was grown first, followed by Au and Ru, and the Ag segments were etched away in nitric acid. This procedure results in a concave shape at the Au ends of the rods. Following electrodeposition, the membrane was dissolved in NaOH solution, and the rods were released and rinsed clean with deionized water.

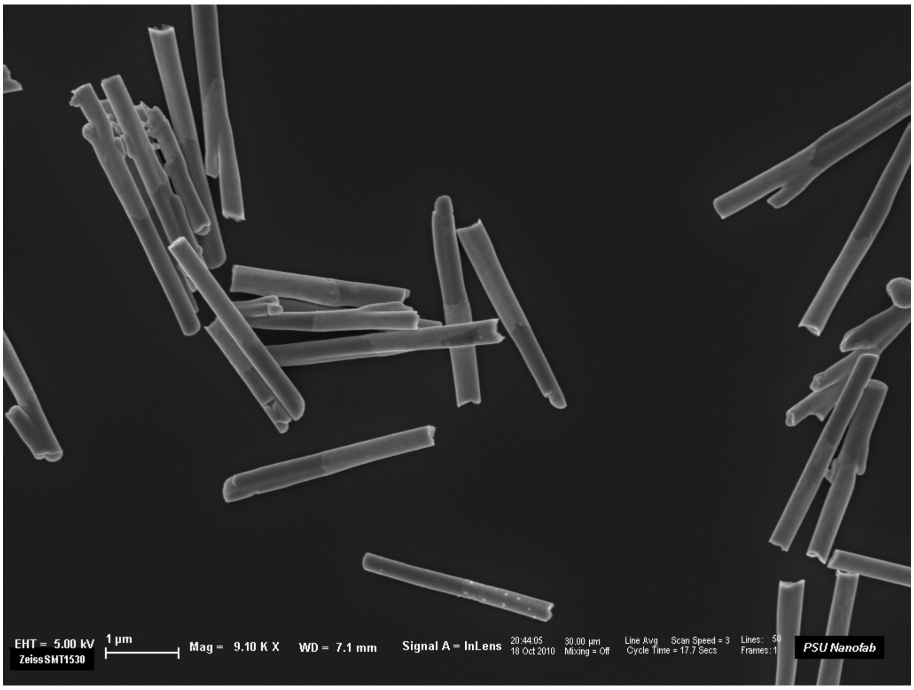

Figure S1. Field-emission scanning electron microscope (FESEM) images of electrodeposited Au-Ru microrods (light segment is gold and dark segment is Ru)

Motor experiments

The microrod suspensions in water were added to H_2O_2 solutions to reach a final concentration of 10%. The suspension was then transferred by capillary action into a capillary tube (VitroCom) that had a rectangular opening with dimensions of 2 mm x 200 μm. The capillary tube was then quickly mounted on top of a silicon wafer by means of a layer of lubricating gel. At the bottom of the silicon wafer we attached a piece of piezoelectric ceramic disk, which was wired to a waveform function generator (Agilent 33210A). The frequency was fine-tuned until resonance was reached in the capillary tube, which was roughly around 3.7 MHz. The ultrasound was switched on and off by tuning the power output of the function generator from

10V to 0V, respectively. The motion capture and tracking analysis were done in the same way as in previous studies.[1-3] The videos were taken at 30 frames per second with an Olympus BX60M microscope in dark field mode.

2. Speeds (in µm/s) of six Au-Ru motors in two propulsion modes

Table S1. Speeds of catalytically powered Au-Ru motors in the presence and absence of acoustic propulsion. The last row represents the speed under acoustic power only, since the chemical and acoustic forces propel in opposite directions.

Motor #	1	2	3	4	5	6
Ultrasound On	65±10	67±8	71±10	64±13	52±8	61±9
Ultrasound Off	35±10	30±8	31±11	34±10	42±13	25±6
Acoustic power only (On+Off)	100±14	97±11	102±15	98±16	94±15	86±11

Note: For each motor at least 50 steps (0.033 second between each step) were tracked to calculate the average speed.

3. Trajectories and speed changes of two Au-Ru motors when ultrasound power was gradually reduced

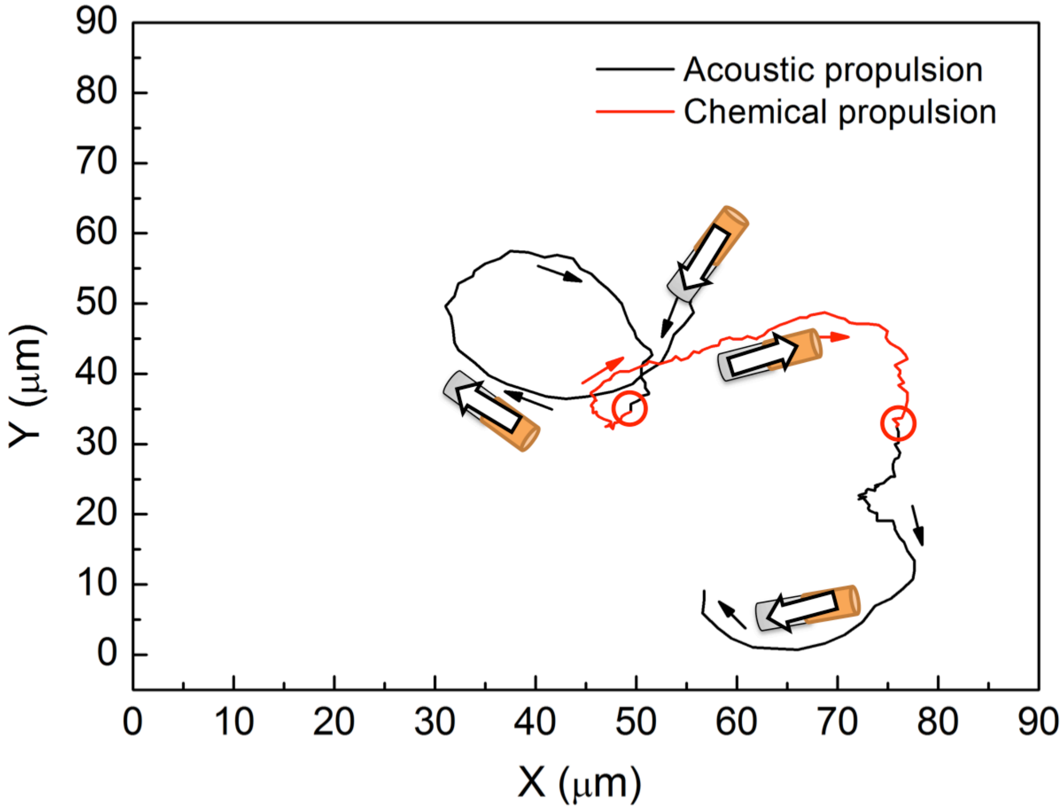

Figure S2. Trajectory of a Au-Ru motor as the acoustic power was decreased and then increased. Red circles mark the spots where the axial movement of the motor is stalled and a crossover between acoustic propulsion and chemical propulsion occurs. Around these points the motor re-orients randomly. Cartoons of Au-Ru motors (Au: gold; Ru: gray) and colored arrows are superimposed to illustrate the direction of movement.

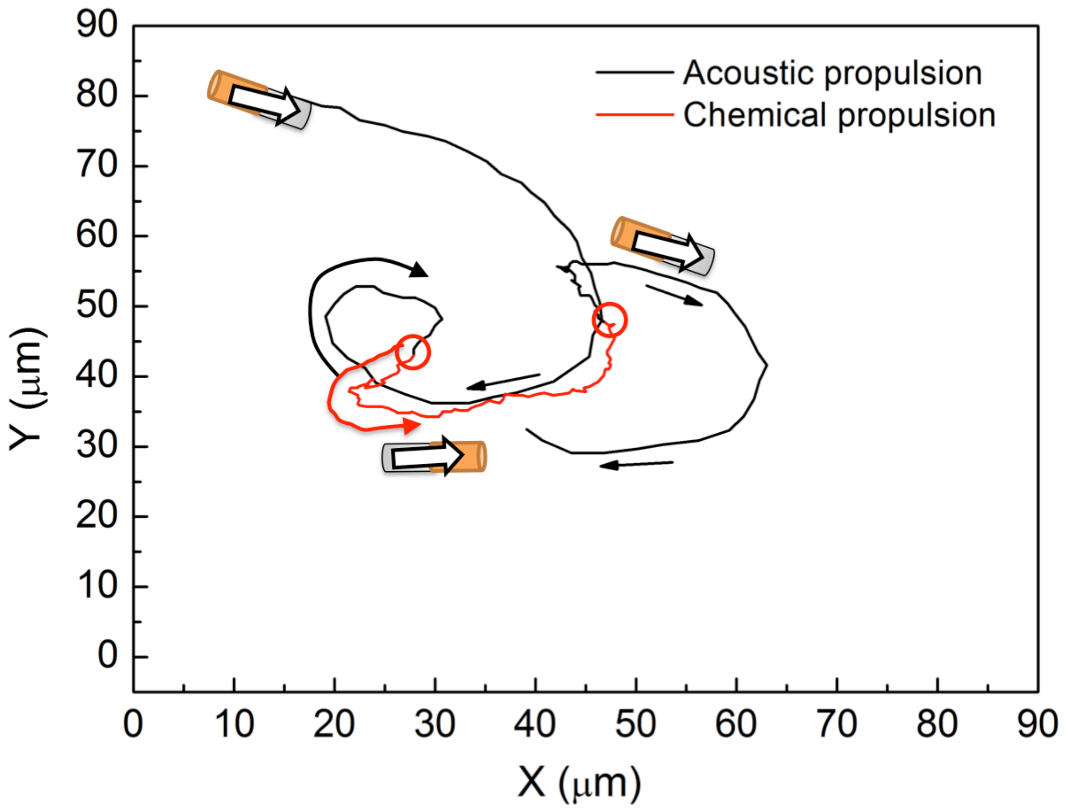

Figure S3 Trajectory of a second Au-Ru motor as the power was decreased and then increased. Red circles mark the spots where the axial movement of the motor is stalled and a crossover between acoustic propulsion and chemical propulsion occurs. Cartoons of Au-Ru motors (Au: gold; Ru: gray) and colored arrows are superimposed to illustrate the direction of movement.

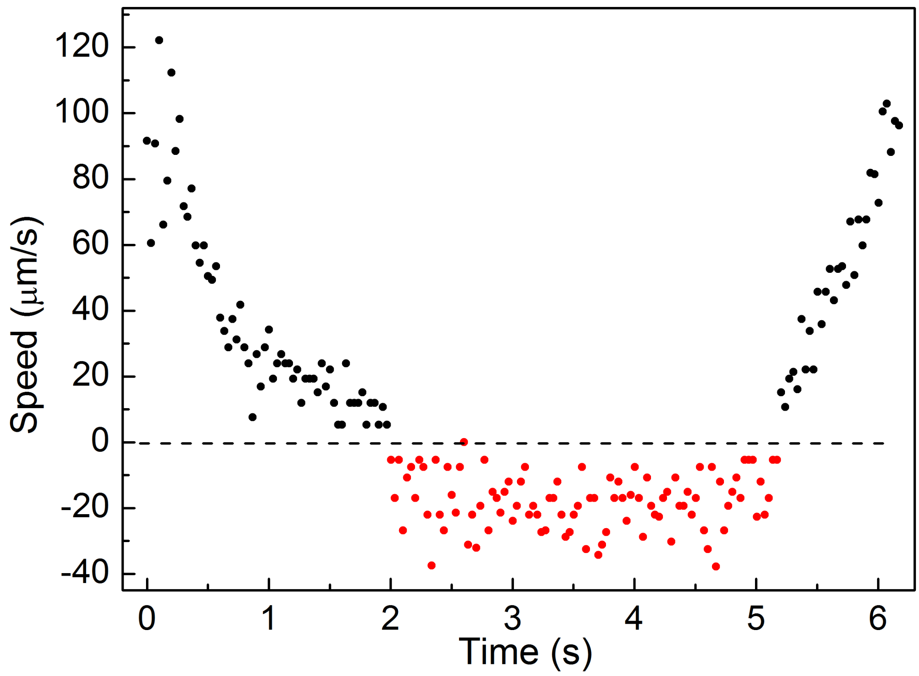

Figure S4. Speed plot as a function of time for the Au-Ru motor tracked in Figure S2. The motor speed gradually decreased as the acoustic power decreased, then was reduced to zero at the crossover point. The forward speed (acoustic propulsion) is shown in black and backward speed (chemical propulsion) is shown in red.

4. Calculation of the width of a band of Au-Ru motors during dispersion

Twelve snapshots were taken from video S6 for data analysis. These snapshots started from when the band was just about to undergo dispersion (right before the ultrasound was turned off, defined as t=0), and the next ten snapshots were taken at 0.3 s time intervals. The final snapshot was taken at t=5.3 s, just before the ultrasound was turned back on again. In each snapshot we divided the image into 30 rectangles along the x axis (a total of 450 pixels, with each pixel corresponding to 0.438 μm), and we used locally written software to locate all the particles in the snapshots (Figure S5).

We then counted how many particles were in each of the rectangle boxes, and plotted the frequency as a function of their position on the x axis. The plot was fitted to a Guassian distribution (Figure S6), and the full width half maximum (FWHM) of the fitting result was used to represent the width of the band in that particular snapshot. The FWHM values of the 12 snapshots were plotted as a function of time in Figure 2b.

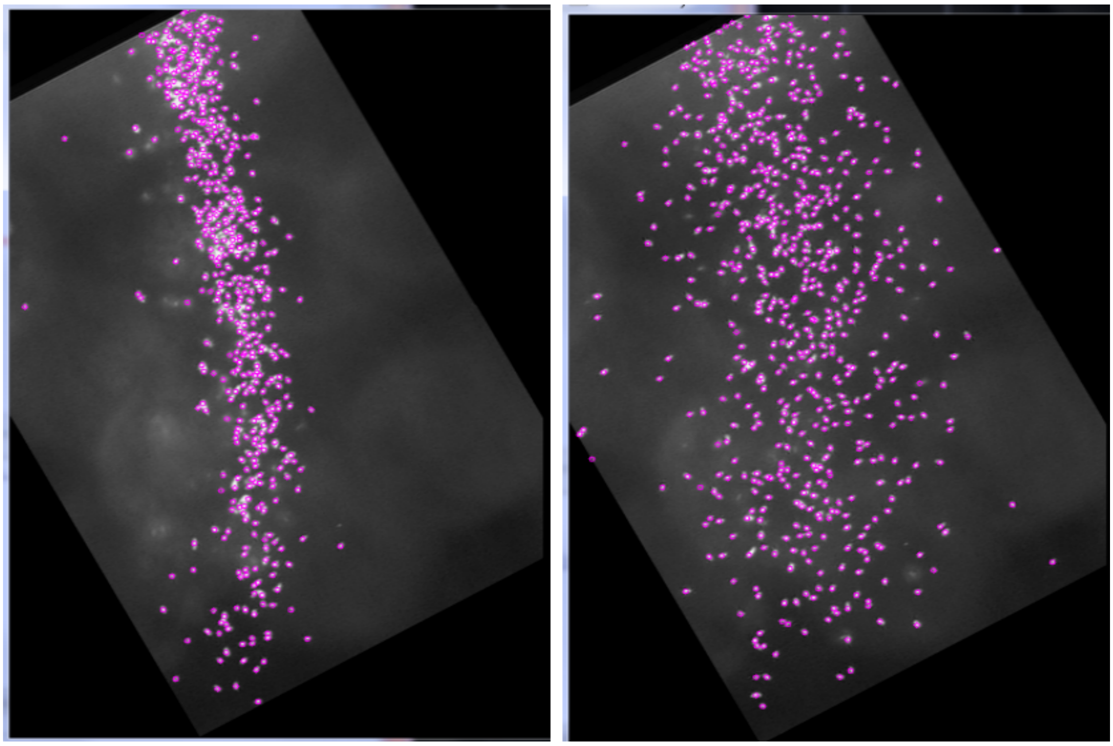

Figure S5. Location of all Au-Ru microrods plotted by the computer program in captured frames at t=0 (left) and t=5.3 s (right). The particles are colored purple by the program, and the images were oriented to align the band vertically.

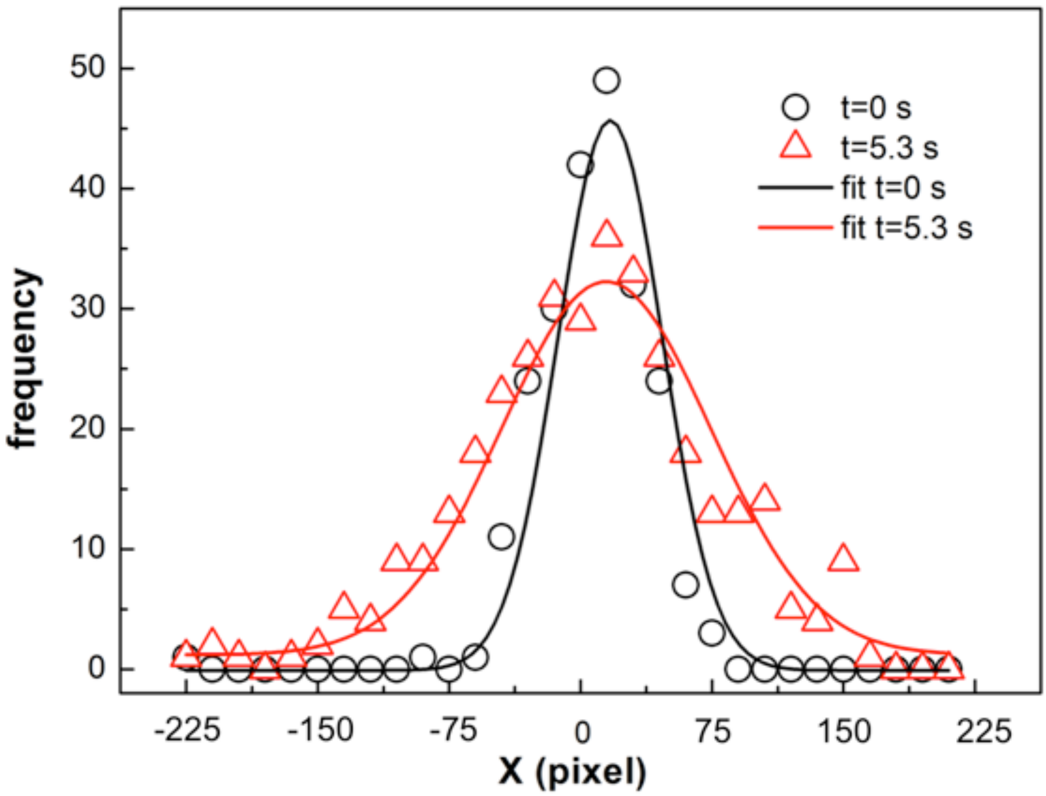

Figure S6. Representative data from the analysis of the dispersion of band structures. Open symbols: counts of particles in a particular rectangle in the image along the x axis at t=0 and t=5.3s; Solid lines: Guassian fits of the two sets of data.

5. Videos

Video S1: Behavior of Au-Ru motors when the acoustic power was rapidly switched. The ultrasound power was turned off around 00:04 in the video, and was later turned on after ~ 1s. This process was repeated for one more time. The video clip was captured in dark field mode at 500X overall magnification.

Video S2: Behavior of Au-Ru motors when the acoustic power was slowly ramped down and then turned up. The motors in the video clip first slow down, then started to move in the opposite direction under chemical propulsion. After the ultrasound resumed full power, the motors switched to acoustic propulsion again. This process was repeated one more time. The video clip was captured in dark field mode at 500X overall magnification.

Video S3: Au-Ru motors propelled entirely by self-electrophoresis in 10% H_2O_2 at the cell bottom in the absence of ultrasound. The video clip was captured in dark field mode at 500X overall magnification.

Video S4: Dispersion of a ring pattern. At the central nodal plane a ring assembled by moving Au-Ru microrods was seen to quickly disintegrate when the ultrasound was turned off (at ~ 00:02), but assembled back into the ring structure when the power was turned back on (at ~ 00:04). The video clip was captured in dark field mode at 200X overall magnification.

Video S5: Dispersion of a chain pattern. At the central nodal plane a spinning chain of Au-Ru microrods was seen to quickly disintegrate when the ultrasound was turned off (at ~ 00:04). The video clip was captured in dark field mode at 200X overall magnification.

Video S6: Dispersion of a band pattern. At the cell bottom Au-Ru motors diffused away from a loose band when the ultrasound was turned off (at ~ 00:01), but aggregated into a band when the sound was turned back on (at ~ 00:06). The video clip was captured in dark field mode at 200X overall magnification.

Video S7: Dispersion of a cluster pattern. At the cell bottom Au-Ru motors diffused away from tight clusters when the ultrasound was turned off (at ~ 00:03), but aggregated into clusters when the sound was turned back on (at ~ 00:06). The video clip was captured in dark field mode at 200X overall magnification.

1 W. Wang, L. A. Castro, M. Hoyos and T. E. Mallouk, *ACS Nano*, 2012, **6**, 6122-6132.

2 W. Wang, W. Duan, A. Sen and T. E. Mallouk, *Proc. Nat. Acad. Sci.* 2013, **110**, 17744-17749.

3 W. Wang, T.-Y. Chiang, D. Velegol and T. E. Mallouk, *J. Am. Chem. Soc.*, 2013, **135**, 10557-10565.